Substituent Effects in Mechanochemical Allowed and Forbidden Cyclobutene Ring-Opening Reactions

Cameron L. Brown,[†] Brandon H. Bowser,[†] Jan Meisner,[‡,δ] Tatiana B. Kouznetsova,[†] Stefan Seritan,[‡,δ] Todd J. Martinez,*[,‡,δ] and Stephen L. Craig*[,†]

[†]Department of Chemistry, Duke University, Durham, North Carolina 27708, United States

[‡]Department of Chemistry and The PULSE Institute, Stanford University, Stanford, California 94305, United States

[δ]SLAC National Accelerator Laboratory, Menlo Park, California 94025, United States

ABSTRACT: Woodward and Hoffman once jested that a very powerful Maxwell demon could seize a molecule of cyclobutene at its methylene groups and tear it open in a disrotatory fashion to obtain butadiene (Woodward, R. B.; Hoffmann, R. The Conservation of Orbital Symmetry. *Angew. Chem., Int. Ed.* **1969**, 8, 781-853). Nearly forty years later, that demon was discovered and the field of covalent polymer mechanochemistry was born. In the decade since befriending our demon, many fundamental investigations have been undertaken to build up our understanding of force-modified pathways for electrocyclic ring-opening reactions. Here, we seek to extend that fundamental understanding by exploring substituent effects in allowed and forbidden ring-opening reactions of cyclobutene (CBE) and benzocyclobutene (BCB) using a combination of single molecule force spectroscopy (SMFS) and computation. We show that while the forbidden ring-opening of *cis*-BCB occurs at a lower force than the allowed ring-opening of *trans*-BCB on the time scale of the SMFS experiment, the opposite is true for *cis*- and *trans*-CBE. Such a reactivity flip is explained through computational analysis and discussion of the so-called allowed/forbidden gap.

Introduction

Electrocyclic reactions have wide utility in both organic synthesis and as the basis for understanding fundamental aspects of chemical reactivity,[1-2] in particular those related to the role of orbital symmetry and concepts of frontier molecular orbital theory. The influence of substituents on electronic structure and reactivity have therefore received much attention. For example, in the paradigmatic conrotatory 4 π-electron ring-opening of cyclobutene (CBE) to 1,3-butadiene, substituents on the ring play a key role in determining thermal barriers to ring opening,[1,3-9] the torque selectivity of the ring opening,[10-12] and the subsequent reactivity of the ring-opened products.[13] Substituents attached to the breaking sigma bond have been shown to perturb the activation energy of the conrotatory ring opening by as much as 7 kcal/mol per substituent.[14] In general, electron donors weaken the adjacent sigma bond and promote outward rotation, whereas strong acceptors favor inward rotation.[9] Substituents attached to the double bond of the cyclobutene ring, on the other hand, typically have a smaller effect (~1-3 kcal/mol) on the barrier to conrotatory ring-opening of CBE.[9] A notable exception is found in benzocyclobutene (BCB), in which case the nascent double bond is also part of an aromatic framework. In general, the CBE ring-opened butadiene product is more stable than the CBE reactant; however, the opposite is true for BCB due to the resulting loss of aromaticity.[15] Additionally, BCBs typically have higher energy barriers to conrotatory ring opening than CBEs.[1,13-16]

Whereas substituent effects have been well documented in the thermally allowed conrotatory ring-opening of CBEs and BCBs,[1,7-8,12] a much smaller set of studies have probed the thermally forbidden disrotatory ring-opening reaction, even in parent reactions.[16-19] The relative dearth of studies is due to the high stereospecificity associated with the conrotatory ring-opening reaction, which makes violations of the so-called Woodward-Hoffmann rules[1] exceedingly rare. A seminal experimental study by Brauman *et al.* on the allowed/forbidden gap ($\Delta G_{A/F}$), i.e. the difference in the activation energies of the symmetry forbidden (disrotatory) and symmetry allowed (conrotatory) reaction, places $\Delta G_{A/F}$ at greater than 15 kcal/mol for a dimethyl-substituted CBE.[20] Lee *et al*. later showed that $\Delta G_{A/F}$ can be altered by introducing planarity constraints on the CBE ring, which decreases favorable orbital interaction between both the σ and π* orbitals and the π and σ* orbitals in the conrotatory transition state.[16] Sakai calculated that the symmetry forbidden disrotatory ring openings of both CBE[17] and BCB[18] proceed through a diradical mechanism, and the calculated $\Delta G_{A/F}$ for BCB (~8 kcal/mol) is found to be 11 kcal/mol lower than $\Delta G_{A/F}$ for CBE (~19 kcal/mol), according to computations at the CAS-MP2/6-31G(d,p) level of theory (**Figure 1**).[18] The calculated transition state structures indicate that lower $\Delta G_{A/F}$ is a result of the disrotatory pathway in BCB retaining aromatic character that is lost at the transition state of the conrotatory pathways. These calculations that directly compare the allowed and forbidden ring-opening pathways for CBE and BCB have yet to be verified experimentally, primarily because the high barriers to classically forbidden reactions limit the toolkit available for their study. Herein we employ covalent polymer mechanochemistry to probe forbidden reactivity and compare experimental reactivities to the computational results (**Figure 1**).

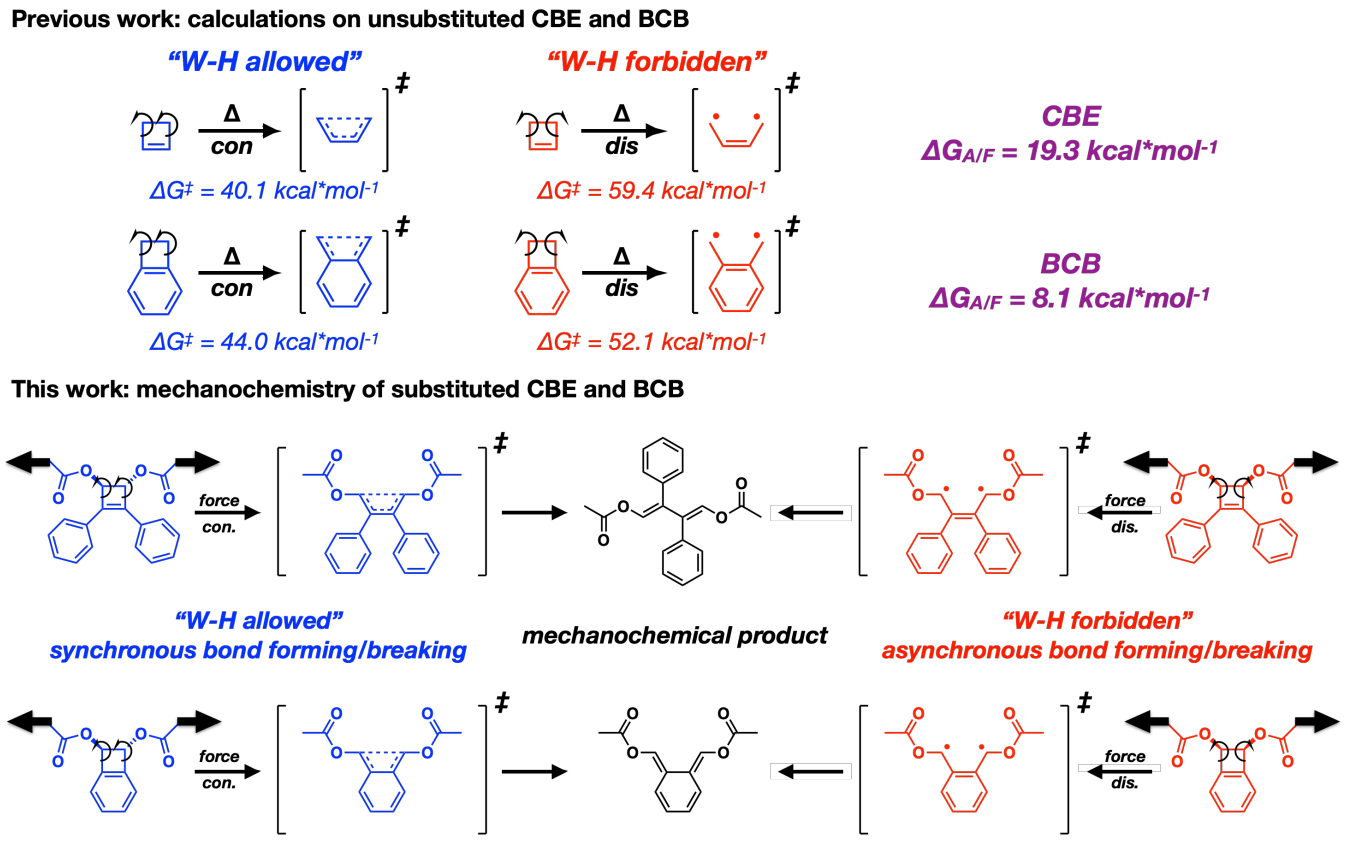

Figure 1. Top: summary of computational findings from Sakai comparing the allowed-forbidden energy gap for thermal ring-opening reaction of CBE and BCB.[17-18] Bottom: summary of key mechanophores and processes that were studied by both SMFS and computational modeling and reported here.

Over the last decade, advances in covalent polymer mechanochemistry have provided a motivation for better understanding symmetry forbidden processes, as well as tools and methods by which that understanding can be obtained. The motivation comes from the fact that coupled mechanical forces can be used to steer electrocyclic reactions down pathways that are opposite to the Woodward-Hoffmann (WH) rules, leading to opportunities in both stress-responsive materials and new chemical reaction manifolds. Moore and co-workers demonstrated that high forces of tension applied to *cis*-diester attachments on BCB forces the reaction mechanism to change from a symmetry allowed thermal conrotatory pathway to a symmetry forbidden thermal disrotatory pathway.[21] This groundbreaking study has been followed by computational[22-29] and experimental[30-33] work aimed at developing a better fundamental understanding of the mechanochemically accelerated reactions of CBE and BCB, and numerous additional examples of analogous apparent violations of orbital symmetry rules have been reported in other systems.[34] At the same time, mechanochemical coupling has provided a means of exploring symmetry forbidden reactivity manifolds that have otherwise remained hidden. For example, Wang *et al.* used single-molecule force spectroscopy (SMFS) experiments to quantify the force-coupled reactivity of a dialkyl-substituted BCB. The force necessary to accelerate the rate constant of the disrotatory ring-opening reaction of *cis*-BCB to ~10 s^{-1} is lower than that required to achieve the same rate in the conrotatory ring-opening reaction of its *trans*-BCB analog (1a).[32] They found that the cross-over force at which *cis*-BCB undergoes a disrotatory ring-opening faster than *trans*-BCB undergoes a conrotatory ring-opening is less than 1370 pN, which is lower than predicted for a dimethyl-substituted BCB system (~1600 pN).[24]

By further applying the SMFS technique, here we systematically explore the differences in both the allowed (conrotatory) and forbidden (disrotatory) reactivity of the CBE and BCB mechanophore systems. We first performed SMFS experiments on the *trans*-CBE and *trans*-BCB mechanophores to probe differences in the allowed pathway, in which electron density shifts in a fully synchronous manner (blue, **Figure 1**). Second, we performed SMFS experiments on the *cis*-CBE and *cis*-BCB mechanophores to probe differences between the forbidden pathways, in which, according to the work of Sakai,[17-18] the electron density shifts asynchronously and there is a buildup of diradical character (red, **Figure 1**). Third, we explore the differences between the allowed and forbidden processes for both CBE and BCB, in order to gain experimental insights into structure-activity relationships that influence $\Delta G_{A/F}$ in 4 π-electron ring-opening reactions. The experimental results are supported by computational studies of the ring-opening reactions using the force-modified potential energy surface (FMPES) approach.[22] The FMPES approach provides activation barriers for ring-opening as a function of force that can be directly compared to the SMFS results. The underlying electronic structure of the force-free and force-coupled reactions are further explored using CASSCF/6-31G* calculations at 0 and 2 nN, respectively. In particular, these calculations provide insight into the degree of synchronicity and diradicaloid character of the allowed and forbidden processes and identify correlations between electronic structure and differences in CBE and BCB reactivity. Fi-

nally, we evaluate the effects of pulling attachments on the allowed and forbidden reactivity, and in particular the force-coupled allowed-forbidden gap, of the BCB mechanophore by comparing SMFS and computational data for diester-BCB to the aforementioned dialkyl-BCB.

Methods

Synthesis of multi-mechanophore containing copolymers

Multi-mechanophore polymers bearing the CBE and BCB units of interest were generated using a tandem ring-closing/ring-opening strategy reported previously (**Figure 2**).[35] The ring closing metathesis (RCM) of bis-alkene functionalized CBE/BCB mechanophores yielded mechanophore-containing macrocycles. The CBE and BCB macrocycles were then copolymerized with freshly distilled 9-oxabicyclo[6.1.0]non-4-ene (epoxy-COD)[36] via ring-opening metathesis polymerization (ROMP) to give multi-mechanophore-containing polymers **P1a**, **P1b**, **P2a**, and **P2b**. Mechanically-inert epoxides were incorporated to increase the adhesion force between the polymer and the tip of the atomic force microscope (AFM) cantilever.[37] Copolymers containing either both *cis*- and *trans*-CBE isomers (**P1c, see SI**) or both *cis*- and *trans*-BCB isomers (**P2c, see SI**) were also synthesized.

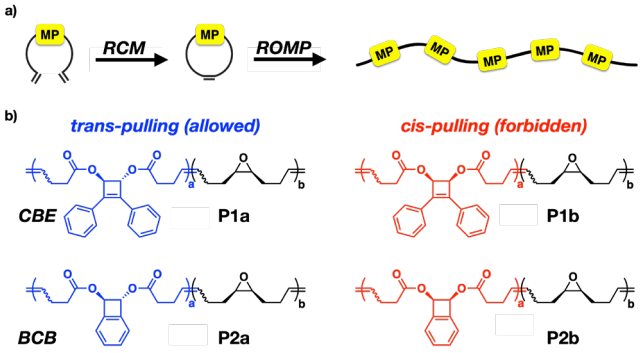

Figure 2. a) Cartoon of the RCM-ROMP synthetic approach. b) Copolymers used in this study, generated from RCM-ROMP.

Single Molecule Force Spectroscopy

The SMFS pulling experiments were conducted in toluene at ambient temperature (~23˚C) in the same manner as described previously,[32,37-39] using a homemade AFM, which was constructed using a Digital Instruments scanning head mounted on top of a piezoelectric positioner, similar to the one described in detail previously.[40] Force curves were collected in dSPACE (dSPACE Inc., Wixom, MI) and analyzed using Matlab (The MathWorks, Inc., Natick, MA). All data were filtered during acquisition at 500 Hz. After acquisition, the data were calibrated and plotted using homemade software written in Matlab language. To obtain the relative extension at the plateaus, the contour lengths of the polymers before and after transition were determined by fitting the pre- and post- transition force curves to an extended freely jointed chain (FJC) model as described previously.[37-38] Such a fit allows the determination of polymer chain lengths corresponding to the initial state, when active mechanophores are intact (*L1*), and the final state, when all mechanophores have undergone an irreversible ring-opening reaction (*L2*).

Experimentally determined values of *L1* and *L2* are compared to modeled values of the contour lengths of the repeating units by a method described previously.[37] The equilibrium conformers of the molecules were minimized at the Molecular Mechanics/MMFF level of theory using Spartan® software.[37] The end-to-end distance of the molecule was constrained until the bonding geometries were noticeably distorted. CoGEF (constrained geometry simulates external force)[41-42] plots of energy vs. displacement were then obtained by varying the constraint in 0.1 Å increments. The incremental change in energy vs. change in distance was taken as the force at the midpoint of the increment, and the resulting force vs. displacement curve was extrapolated to zero force to give a force-free contour length (L_{RC} or L_{RO}) of the computational polymer fragment where RC and RO stand for ring-closed and ring-opened respectively. $L_{epoxy\ COD}$ was determined previously to be 9.30 Å.[32] The ratio of polymer contour lengths, *L2*/*L1*, are obtained from the following equation:

$$\frac{L2}{L1} = \frac{(L_{RO} \times \chi_{RO}) + (L_{epoxy\ COD} \times \chi_{epoxy\ COD})}{(L_{RC} \times \chi_{RC}) + (L_{epoxy\ COD} \times \chi_{epoxy\ COD})}$$

where χ denotes the mole fraction of a particular repeating unit (as determined by ^{1}H-NMR spectroscopy), and *L* refers to the end-to-end distance obtained from CoGEF calculations for the corresponding repeat.

Computational Modeling

Free energy barriers were calculated using force-modified potential energy surfaces (FMPES).[22] The B3LYP density functional and the 6-31G* basis set were used and compared to wave function-based methods,[43-47] see SI for further information. We demonstrate the influence of solvation to be negligible (see SI) due to the unipolar nature of toluene, therefore all calculations are performed in the gas phase. Forces were applied to the outermost carbon atoms of the model mechanophores. In previous studies this model has proven to be effective in assessing the mechanochemical reactivity of mechanophores embedded within polymers.[26,48] For the conrotatory ring-opening of *trans*-substituted CBEs and BCBs, reactants and transition structures are optimized on the force-free PES and on FMPES in steps of 0.5 nN. At forces above a critical value (4.0 nN for *trans*-BCB, 3.0 nN for *cis*-BCBs, and 3.5 nN for *cis*- and *trans*-CBEs), the reactants have no stable minimum structures on the respective FMPES; in other words, immediate (barrierless) ring-opening would occur at these forces. For the disrotatory ring-opening of *cis*-substituted CBEs and BCBs, transition state optimization below 0.5 nN (1.0 nN for CBE) converged to the conrotatory transition structure, indicating that there is no first-order saddle point associated with this reaction channel.[16] For the conrotatory ring-opening of *cis*-substituted CBEs and BCBs, transition states have been optimized below a system-dependent critical force at which the first-order saddle point associated with this reaction channel disappears.[23-24] At these threshold forces (> 0.5 nN for alkyl-BCB, > 1.0 nN for ester-BCB, and > 2.5 nN for CBE), the topology of the FMPES changes significantly, which will be the subject of future computational studies.

For the calculation of the natural orbitals along the reaction pathways, complete-active-space self-consistent field (CASSCF) calculations have been performed (see SI for further information). The effective number of unpaired electrons (ENUE) is calculated according to

$$N = \sum_{i=1}^{m} n_i^2 (2 - n_i)^2$$

where n_i is the natural orbital occupation number of the active orbital i.[49] Closed and unoccupied (virtual) orbitals do not contribute to the ENUE.

Results and Discussion

Woodward-Hoffman Allowed *trans*-pulling

Figure 3(a-b) shows experimental force versus separation curves for polymers **P1a** and **P2a**, containing *trans*-CBE and *trans*-BCB mechanophores, respectively. Each plateau can be characterized by a single force, f^*, determined by taking the second derivative of the force-separation curve and finding the inflection point. The plateau and its corresponding f^* reflect the force required to mechanically accelerate the half-life of the CBE and BCB ring-opening reactions to approximately ~ 100 ms, and values of f^* are consistent across all the pulls of a given type of polymer gathered over several days and multiple cantilevers. In this way, f^* was determined to be 1270 pN and 1490 pN for polymers **P1a** and **P2a**, respectively (**Table 1**). The mechanically induced plateaus can be further characterized by the ratio *L2*/*L1*, where *L2* is the polymer contour length after mechanical activation and *L1* is the polymer contour length before mechanical activation. This ratio is a function of the change in contour length of each mechanophore repeat and the relative ratio of mechanophore to epoxy-COD repeat. By pulling on a *trans*-substituted CBE or BCB mechanophore, the mechanical work is directly coupled to the thermally-allowed conrotatory ring-opening pathway, and thus the *E,E*-ring-opened products are expected.

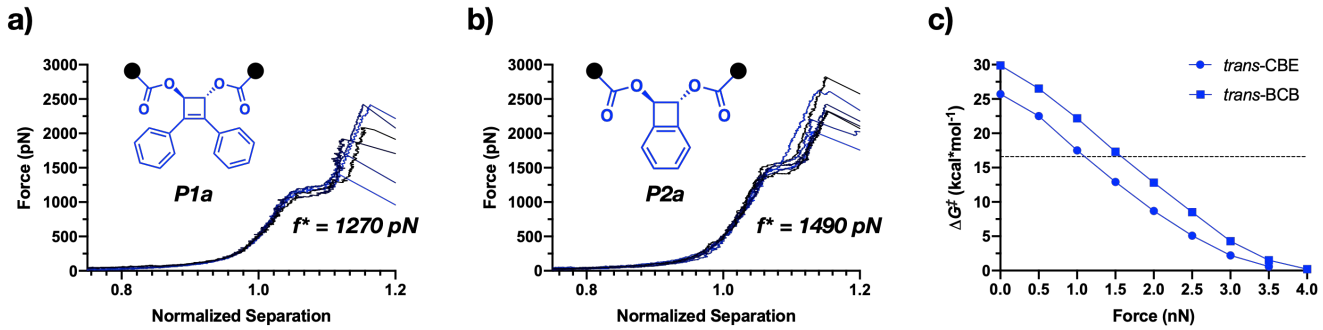

Figure 3. Overlay of several force vs. separation curves for copolymers **P1a** (a) and **P2a** (b). The curves were normalized to have the same separation at a force of 500 pN. The reported f^* is an average of several curves and was determined according to the process described in the methods section. (c) Activation barriers as a function of force for both trans-CBE (circles) and trans-BCB (squares) mechanophores, calculated as described in the methods section. The dotted line represents the activation barrier for a generic chemical reaction that has a rate constant of 10 s^{-1} at 298K, which is a reasonable approximation for the rate of ring-opening of the mechanophores during SMFS experiments.

Table 1. Plateau force corresponding to mechanochemical CBE/BCB ring-opening (f^*), calculated conrotatory (con) and disrotatory (dis) ring-opening activation energies ($\Delta G^{\ddagger}$) at F = 0 nN and F = 2 nN, percent of polymer repeating units containing either CBE or BCB, and the ratio of polymer contour length before and after mechanochemical activation (L2/L1) by fitting with a freely-jointed chain model (FJC), and theoretical L2/L1 ratios by modeling if all ring-opened products are the *E,E*-isomer and if all ring-opened products are the *E,Z*-isomer.

Polymer	f^* (pN)	$\Delta G^{\ddagger}_{F=0}$ (con)	$\Delta G^{\ddagger}_{F=2}$ (con)	$\Delta G^{\ddagger}_{F=2}$ (dis)	%CBE/BCB	L2/L1 (FJC)	L2/L1 (Model-*E,E*)	L2/L1 (Model-*E,Z*)
P1a	1270	25.7	8.7	---	21%	1.07	1.05	1.03
P1b	1520	31.7	---	10.1	18%	1.08	1.05	1.04
P2a	1490	29.9	12.8	---	29%	1.05	1.05	1.02
P2b	1040	38.7	---	3.9	22%	1.05	1.05	1.03

The *trans*-CBE-containing copolymer (**P1a**) and *trans*-BCB-containing copolymer (**P2a**) were synthesized as described above, and the percent incorporation of mechanophore was determined by ^{1}H-NMR to be 21% and 29% respectively. According to CoGEF calculations,[41-42] **P1a** is expected to undergo approximately a 5% elongation if the *E*,*E*-isomer is the sole ring-opened product and approximately a 3% elongation if the *E*,*Z*-isomer is the sole ring-opened product. Similarly, **P2a** is expected to undergo approximately a 5% elongation (*E*,*E*-isomer) and 2% elongation (*E*,*Z*-isomer). The average observed elongations by SMFS for **P1a** and **P2a** (7% and 5% respectively) is thus more consistent with the mechanically generated *E*,*E*-ring-opened product expected from the "WH-allowed", conrotatory ring-opening (see SI for details).

Figure 3c shows plots of computationally determined B3LYP FMPES activation energies ($\Delta G^{\ddagger}$) as a function of applied force for *trans*-substituted CBE and BCB mechanophores. Initially, the force-free $\Delta G^{\ddagger}_{con}$ of *trans*-CBE (25.7 kcal/mol) is ~4 kcal/mol lower than that of *trans*-BCB (29.9 kcal/mol). In general, BCB ring systems tend to be less thermally reactive than analogous CBE ring systems due to the loss of aromaticity in the *o*-QDM products, which slows down the ring-opening of BCB.[16,18] As the applied mechanical force via the *trans*-attachments increases, $\Delta G^{\ddagger}_{con}$ decreases at relatively the same rate in both cases and the energy gap between them does not change significantly until higher forces are experienced (>3.0 nN). This suggests that the mechanical coupling is similar for both systems at the forces that correspond to reactivity on the time scale of the SMFS experiment.

The point where the curve intersects the black dotted line in **Figure 3c** represents the force at which the activation barrier is lowered to ~16.6 kcal/mol, which corresponds to a rate constant for ring-opening that would lead to a typical plateau extension in the SMFS experiments (~10 sec^{-1}). This force therefore reflects the value of f^* expected solely on the basis of the FMPES computations. **Figure 3c** indicates that this calculated force is lower for the *trans*-CBE mechanophore (1.10 nN) than that of the *trans*-BCB mechanophore (1.60 nN), and these computational results are qualitatively consistent with our experimental SMFS results for **P1a** and **P2a.** Because the rates at which the activation barriers change as a function of force are similar (below 3 nN), these observed differences in force-coupled reactivity are primarily attributed to differences in the intrinsic ring-opening reactivity of CBE and BCB, as opposed to differences in the mechanical coupling.

Woodward-Hoffman Forbidden *cis*-pulling

Figure 4a-b shows experimental force versus separation curves for **P1b** and **P2b**, containing *cis*-CBE and *cis*-BCB mechanophores, respectively. Using the same approach as in the *trans*-substituted case, f^* was determined to be 1520 pN for **P1b** and 1040 pN for **P2b** (**Table 1**). These experimental observations correspond well to the values of 1.54 nN and 1.04 nN, respectively, expected based on FMPES calculations (**Figure 4c**). In contrast to the *trans*-substituted mechanophores, where the thermally allowed conrotatory reaction was mechanically induced, early work on stretching *cis*-substituted CBE or BCB mechanophores has shown that mechanical work can directly couple to the thermally forbidden disrotatory ring-opening pathway to give the *E,E*-ring-opened products.[21-24] Recently however, Tian *et al.* have reported that for (*Z*)-2,3-diphenylcyclobutene-1,4-dicarboxylate, low forces also mechanically accelerate the conrotatory reaction and a mixture of *E,E* and *E,Z* products were observed.[50] Such a mixture is consistent with the FMPES results for CBE/BCB below ≈1 nN force, as shown in **Figure 4c**.

cis-CBE-containing copolymer (**P1b**) and *cis*-BCB-containing copolymer (**P2b**) were synthesized according to the above procedure, and the percent incorporation of mechanophore was determined by ^{1}H-NMR to be 18% and 22% respectively. Upon application of force, **P1B** is expected to elongate by approximately 5% if the *E*,*E*-isomer is the sole ring-opened product and by approximately 4% if the *E*,*Z*-isomer is the sole ring-opened product by CoGEF calculations. Similarly, **P2B** is expected to elongate by approximately 5% if the *E*,*E*-isomer is the sole ring-opened product and by approximately 3% in the *E*,*Z*-isomer is the sole ring-opened product. The average observed elongation by SMFS was 8% and 5% for **P1B** and **P2B** respectively. Based on these observations it is likely that these systems are dominated by the disrotatory ring-opening mechanism; however, we cannot rule out the presence of some conrotatory ring-opening as well due to the relatively small changes in contour length of these polymers (see SI for details). Even if the two processes were equal contributors, the kinetics in this force regime would only overestimate the rate of the disrotatory reaction by a factor of 2, and we therefore treat the observed kinetics as a reliable reflection of the force-coupled energetics of the forbidden process.

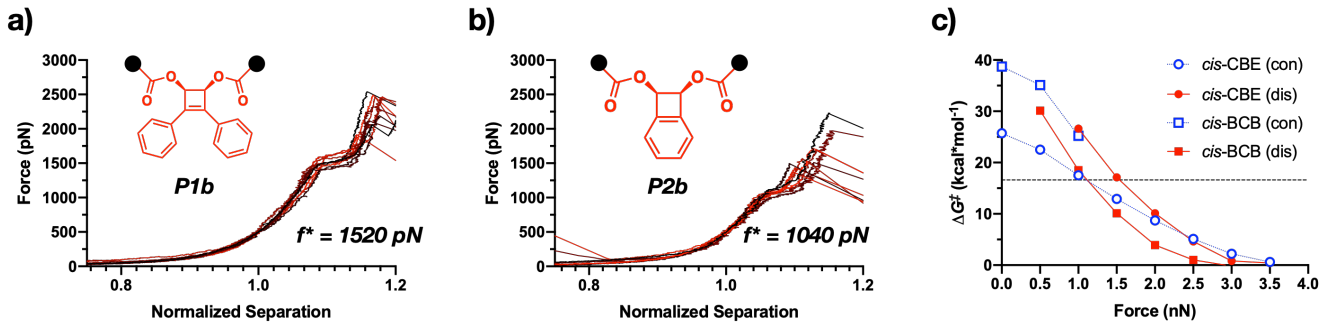

Figure 4. Overlay of several force vs. separation curves for copolymers **P1b** (a) and **P2b** (b). The curves were normalized to have the same separation at a force of 500 pN. The reported f^* is an average of several curves and was determined according to the process described in the methods section. (c) Activation barriers as a function of force for both cis-CBE (circles) and *cis*-BCB (squares) mechanophores, calculated as described in the methods section. The dotted line represents the activation barrier for a generic chemical reaction that has a rate constant of 10 sec^{-1} at 298 K, which is a reasonable approximation for the rate of ring-opening of the mechanophores during SMFS experiments.

In general, the barriers for conrotatory ring-opening of *trans*-cyclobutenes are greater than those of their *cis*-substituted analogs, primarily as a result of increased steric hindrance.[1,51-52] Such is the case here as well; $\Delta G^{\ddagger}$ for the force-free conrotatory ring opening of *cis*-substituted CBE and BCB is calculated to be 31.7 and 38.7 kcal/mol, respectively (**Figure 4c**), and these barriers are both several kcal/mol higher than those of their trans analogs. In comparing the computational results for the two mechanophores, each of *cis*- and *trans*-CBE has a lower conrotatory $\Delta G^{\ddagger}$ than its corresponding BCB isomer, as expected due to the loss of aromaticity in the ring opening of BCB. Similar to a recent report by Tian *et al.*,[50] we find that application of mechanical force across *cis*-CBE and *cis*-BCB changes the potential energy landscape such that two competing ring-opening processes exist at low forces, a classically allowed conrotatory path and a classically forbidden disrotatory path. Computationally, the disrotatory pathways do not exhibit well-defined transition states until 1.0 nN for *cis*-CBE and 0.5 nN for *cis*-BCB. As external force is increased, the energy barriers for both conrotatory and disrotatory ring-opening processes decrease. At forces above 1.0 nN the conrotatory path for *cis*-BCB cleanly disappears, leaving only the disrotatory path. In contrast, the reaction of *cis*-CBE involves competitive conrotatory and disrotatory pathways until the conrotatory barrier disappears at 2.5 nN, at which point the calculated overall energy barrier is virtually non-existent.

Both the conrotatory and disrotatory ring-opening force-modified potential energy surfaces have similar energetics

around the point expected to correspond with the timescale of the SMFS experiment (**Figure 4c**). At this intersection (black dotted line), the expected activation force of 1.54 nN is consistent with our SMFS observations (f^* ~ 1.52 nN). The disappearance of competing saddle points and importance of reaction dynamics in determining product distribution is an interesting and increasingly observed phenomenon in force-coupled reactions.[48,50,53] As discussed in the previous paragraph, a distinct transition state for conrotatory *cis*-CBE ring-opening disappears on the FMPES at forces less than those required to reach the energy barrier where chain extension competes with tip-stage displacement in the SMFS experiment. The disrotatory ring-opening pathway, however, remains, and its expected activation force of 1.04 nN is also consistent with our experimental observations from SMFS (f^* ~ 1.04 nN).

For the CBE and BCB systems described here, CASSCF calculations were used to determine the natural orbital occupancy numbers along the force-free and force-modified reaction pathways for each cyclobutene isomer pair (**Figure 5a**). Both *trans* isomers undergo an allowed conrotatory ring-opening with a maximum effective number of unpaired electrons (ENUE) of ~0.5. Interestingly, the maximum ENUE along the conrotatory pathway slightly increases as a function of force, as shown in **Figures 5b-c**. For the *cis* isomers, CASSCF calculations indicate that the forbidden disrotatory ring-opening processes have peak ENUEs of ~2, caused by the crossing of natural orbitals at this point and consistent with a diradical mechanism. With increasing force, the position of the transition state shifts toward the reactants (earlier along the reaction coordinate), and the ENUE maxima along the disrotatory reaction paths are located after the transition state structure along the reaction coordinate, which is also in accordance with the observations of the disrotatory ring-opening of CBE by Kochar et al.[25]

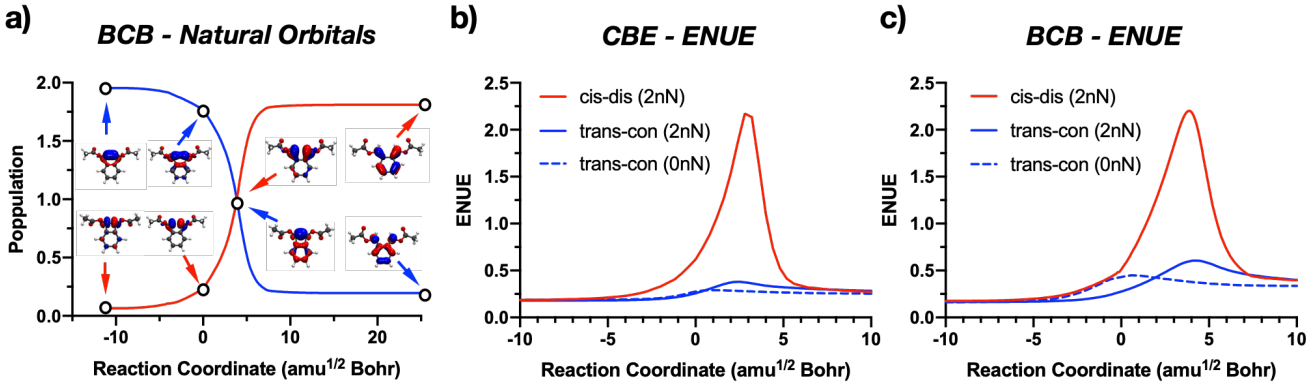

Figure 5. a) *cis*-BCB natural orbitals from CASSCF along the B3LYP 2.0 nN FMPES disrotatory reaction coordinate. Here, just the two natural orbitals with occupation numbers that cross after the transition state are shown. The points indicate structures of reactant, transition state, point of highest diradical character, and product, respectively. b) and c) effective number of unpaired electrons along respective reaction coordinates of CBE and BCB ring-opening, respectively. For the disrotatory ring opening reactions of the *cis*-substituted CBE and BCB, the ENUE maximum is caused by the crossing of natural orbital occupation numbers.

CBE vs BCB and the allowed/forbidden gap

Figure 6a-b shows representative force versus separation curves for copolymers **P1c** and **P2c**, which contain a mixture of *cis*- and *trans*- isomers of CBE and BCB mechanophores, respectively. Consistent with what was observed for the "pristine" copolymers described above, for the mixed copolymers the *trans*-CBE mechanophores activate at a lower f^* than *cis*-CBE mechanophores, and conversely the *cis*-BCB mechanophores activate at a lower f^* than the *trans*-BCB mechanophores. We explain this "flip" in force-modified reactivity by considering both electronic and mechanical effects.

Initially, the calculated force-free activation energy ($\Delta G^{\ddagger}$) of the disrotatory mechanism for both *cis* mechanophores is higher than the $\Delta G^{\ddagger}$ of the conrotatory mechanism for both of the corresponding *trans* mechanophores. As the applied force is increased, the energy barriers for *cis* mechanophores decrease more quickly than the energy barriers for *trans* mechanophores, and each mechanophore pair exhibits a cross-over force, above which the energy barrier for the disrotatory ring-opening of the *cis* mechanophore is lower than that of the conrotatory ring-opening of *trans* mechanophores (**Figure 6c-d**). The calculated cross-over force for CBE is ~2.36 nN, well above the force necessary to reach the ~16.6 kcal/mol barrier probed in the SMFS experiment (black line). In contrast, the calculated cross-over force for BCB is ~0.74 nN, which is less than the force relevant to SMFS.

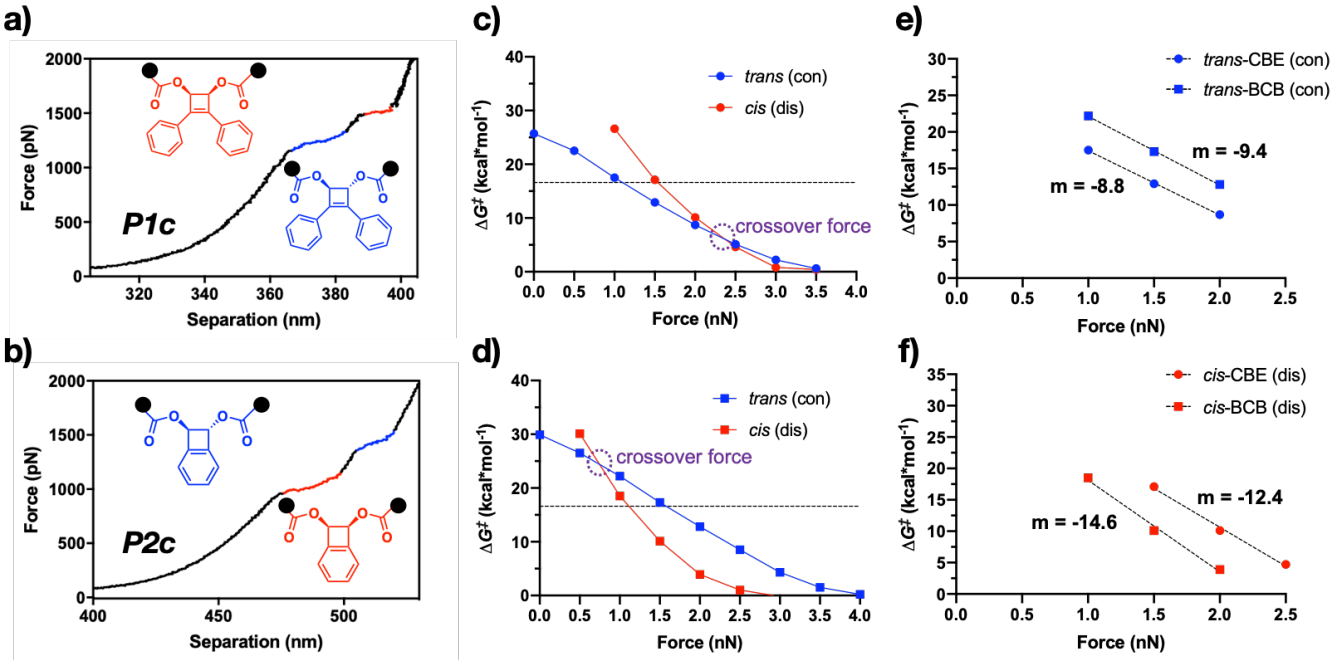

Figure 6. a) SMFS of copolymer **P1c**, which contains both *cis* and *trans* CBE monomers. b) SMFS of copolymer **P2c**, which contains both *cis* and *trans* BCB monomers. c) Activation energy as a function of force for both *cis* (red) and *trans* (blue) CBE. d) Activation energy as a function of force for both *cis* (red) and *trans* (blue) BCB. The dotted line in both c) and d) represents the activation barrier for a generic chemical reaction that has a rate constant of 10 sec^{-1} at 298K, which is a reasonable approximation for the rate of ring-opening of the mechanophores during SMFS experiments. e-f) Plots showing the dependence of $\Delta G^{\ddagger}$ on applied force for the allowed (e) and forbidden (f) processes across the force ranges relevant to the SMFS experiment. Slopes from linear fits ($m_{BCB/CBE}$) are provided.

The combined computational and experimental data can be used to assess how the structural change on going from CBE to BCB influences the allowed-forbidden gap $\Delta G_{A/F}$. Because their structures and reaction paths are quite similar, the *cis*-CBE and *cis*-BCB mechanophore reaction paths are expected to be coupled in nearly identical ways to the applied force. This expectation is borne out by the computations, which show that the force coupled change in the activation energy of the forbidden process, $(\Delta G^{\ddagger}/df)_F$, is -20.0 and -16.5 kcal mol^{-1} nN^{-1} for BCB and CBE, respectively, across the force ranges relevant to SMFS (**Figure 6f**). The corresponding values $(\Delta G^{\ddagger}/df)_A$ for the allowed processes are -9.4 and -9.6 kcal mol^{-1} nN^{-1} (**Figure 6e**). The difference in allowed-forbidden gap can then be estimated as follows:

$$\Delta G^{\ddagger}_{A/F} = \left(f^{*}_{F(CBE)} - f^{*}_{F(BCB)}\right) \cdot (\Delta G^{\ddagger}/df)_F - \left(f^{*}_{A(CBE)} - f^{*}_{A(BCB)}\right) \cdot (\Delta G^{\ddagger}/df)_A$$

We then take the average of the computed $(\Delta G^{\ddagger}/df)_F$ and $(\Delta G^{\ddagger}/df)_A$, along with the experimental plateau forces f^* obtained from **Table 1**, to obtain a difference in allowed-forbidden gap of -10.9 kcal/mol. In other words, $\Delta G_{A/F}$ of the force-coupled BCB ring opening is about 11 kcal/mol lower than that of CBE. This difference is in good agreement with prior work by Sakai, who calculated that $\Delta G_{A/F}$ for unsubstituted BCB (~8 kcal/mol) is lower than $\Delta G_{A/F}$ for unsubstituted CBE (~19 kcal/mol) by 11 kcal/mol.[17-18] The difference in the two processes is attributed to the fact that the symmetry forbidden disrotatory ring-openings of both unsubstituted CBE[17] and unsubstituted BCB[18] proceed with more substantial diradical character than the allowed analogs, also supported by our calculations.

Without the influence of an external force, the conrotatory ring-opening of BCB is less favored than the ring-opening of CBE due to the loss of aromaticity, thus leading to a higher free energy barrier. For the disrotatory ring-opening of both CBE and BCB, however, the aromaticity of the benzene ring of BCB remains intact at the transition state,[18] and the loss of aromaticity lags the formation of diradical character. In fact, the breaking of aromaticity is accompanied by the recombination of the two unpaired electrons with the existing pi-system. Thus, dearomatization is not a substantial contributor to the energy barrier of the disrotatory ring opening, despite being responsible for the higher conrotatory ring opening energy barrier of BCB than CBE.[17-18] Instead, the main contribution to the potential energy barrier of the disrotatory processes stems from homolytic scission of the C-C sigma bond. BCB likely has a lower barrier for this C-C bond breaking due to its greater ring strain relative to CBE.

Ester vs alkyl handles

The above contributions of *cis* and *trans* pulling on CBE and BCB mechanophores are evaluated in the context of ester attachments linking the mechanophores to the stretched polymer chain, but the nature of that substituent can have an impact on both the force-free reactivity and the mechanical coupling. We next consider the effect of an ester vs. an alkyl attachment on BCB ring opening, by comparing the results above with previous SMFS studies of an alkyl-substituted BCB system.[32] In that study, the *cis*-BCB mechanophore opens at a lower force (f^* ~ 1370 pN) than the allowed transition of the *trans*-BCB (f^* ~ 1500 pN), as also observed for the ester attachment studied here (1040 and 1490 pN, respectively).[32] Interestingly, the force gap between the alkyl-substituted *cis*- and *trans*- BCB is only ~130

pN, in comparison to the ~450 pN force gap observed here in the corresponding ester-substituted BCBs (**Table 1**).

The greater reactivity of *cis*- relative to *trans*-BCB in the force-coupled reactions of ester vs. alkyl substituted BCB is due to mechanical, rather than (or in spite of) intrinsic electronic effects. **Figure 7** shows plots of the calculated $\Delta G^{\ddagger}$ vs applied force for *cis*/*trans* alkyl-substituted BCB mechanophores, analogous to the calculations for ester-substituted CBE and BCB reported above. The force-free activation energy ($\Delta G^{\ddagger}$) of *trans*-alkyl BCB is ~6 kcal mol^{-1} higher in energy (36.1 kcal mol^{-1}) than that of *trans*-ester BCB (29.9 kcal mol^{-1}). Such stabilization is consent with the findings of Niwayama *et al*., who found that electron donating substituents lower the activation barrier of the conrotatory ring-opening of cyclobutenes.[9] As more force is applied across the *trans* attachments, however, the difference in activation energies shrinks until it is virtually identical at the transition force required for activation on the timescale probed in the SMFS experiment, which is in line with our experimental results (f^* = 1500 vs. 1490 pN for alkyl and ester attachments). The enhanced mechanical leverage of dialkyl relative to diester attachments is consistent with calculations reported previously by Tian *et al*. on *trans*-cyclobutene derivatives.[54]

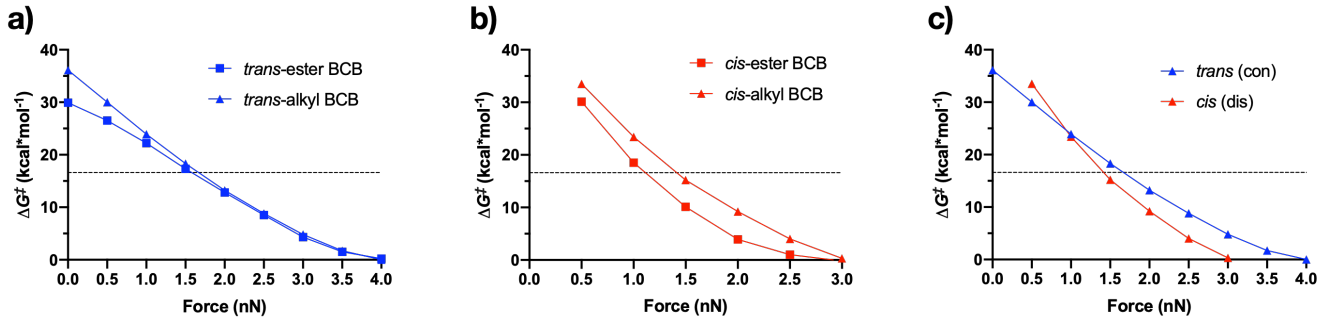

Figure 7. a) Activation barriers as a function of force for both *trans*-ester BCB (blue squares) and *trans*-alkyl BCB (blue triangles) mechanophores, calculated as described in the methods section. b) Activation barriers as a function of force for both *cis*-ester BCB (red squares) and *cis*-alkyl BCB (red triangles) mechanophores. c) Activation energy as a function of force for both *cis* (red) and *trans* (blue) alkyl BCB. The dotted line represents the activation barrier for a generic chemical reaction that has a rate constant of 10 sec^{-1} at 298K, which is a reasonable approximation for the rate of ring-opening of the mechanophores during SMFS experiments.

As with the *cis*-ester BCB, the *cis*-alkyl BCB does not have a computational first-order saddle point for disrotatory ring opening at 0 nN, but the trends in reactivity as a function of force provide some insight. In particular, we note that in contrast to the *trans*-BCBs, the *cis*-ester BCB is accelerated more with increasing force than is the *cis*-alkyl BCB. The two derivatives are similar in reactivity at low force, but the ester is more reactive at high force. In other words, at low force the preference for the allowed pathway is greatest for the diester BCBs, but the preference diminishes with increasing force more rapidly for the ester substituents and ultimately reverses at lower force than in the dialkyl analogs.

Conclusion

In summary, we have quantified force-coupled reactivity of CBE and BCB along conrotatory and disrotatory pathways via single molecule force spectroscopy. These experimental results provide an important benchmark for calculations, and the agreement supports the validity of the computational methodology for these and similar reactions going forward. The results provide insights into the energetics of allowed and forbidden reactivity, and the difference in the so-called allowed/forbidden gap for BCB is lower than CBE, as inferred from force-coupled reactions. Similar methodology could be used for other structure-reactivity relationships in CBEs or related reaction classes.

In addition to the electronics of the conjugated π system, substituent effects at the pulling attachment are shown to be important, with *trans*-alkyl handles providing more mechanical leverage than *trans*-ester handles in conrotatory reactions, while *cis*-ester handles provide more mechanical leverage than *cis*-alkyl handles in disrotatory reactions. Understanding these various influences is important beyond just understanding fundamental questions of reactivity, because mechanophores that react through electrocyclic reactions are of increasing interest for applications such as self-healing/strengthening,[55-57] stress-reporting,[58-62] and mechanoacid generation.[34,63-64] We speculate that mechanophores that react via forbidden pathways are especially intriguing, because forbidden reactions are intrinsically more inert in the absence of force than their allowed counterparts, but (as observed here for the BCB mechanophore) they can outpace the competing allowed reactions at forces relevant to mechanochemical response. For example, replacing alkyl handles with ester handles, as shown here, both slows the force-free reaction and accelerates the force-coupled reaction. Additional studies of substituent effects on competing force-coupled reaction pathways are therefore likely to be quite productive.

ASSOCIATED CONTENT

Supporting Information.
The Supporting Information is available free of charge via the Internet at http://pubs.acs.org.

Experimental Procedures, spectroscopic data, SMFS, and computational details (PDF)

AUTHOR INFORMATION

Corresponding Author

* stephen.craig@duke.edu
* todd.martinez@stanford.edu

Present Addresses

Cameron L. Brown – Eastman Chemical Company, 200 South Wilcox Drive, Kingsport, TN, 37660

Author Contributions

The manuscript was written through contributions of all authors. All authors have given approval to the final version of the manuscript.

Funding Sources

National Science Foundation grants CHE-1808518 (to S.L.C.) and DGE-1106401 (to C.L.B.). Duke University (Dean's Graduate Fellowship to C.L.B.). U.S. Army Research Office under grant W911NF-15-1-0525 (to T.J.M.).

Notes

The authors declare no competing financial interest.

ACKNOWLEDGMENT

This material is based on work supported by the National Science Foundation under grant CHE-1808518 (to S.L.C.) and the U.S. Army Research Office under grant no. W911NF-15-1-0525 (T.J.M.). C.L.B. acknowledges support from the National Science Foundation Graduate Research Fellowship Program to C.L.B. under grant no. DGE-1106401 and the Dean's Graduate Fellowship from Duke University. J.M thanks the Dr.-Leni-Schöninger foundation and the Deutsche Forschungsgemeinschaft (project number 419817859) for financial support.

ABBREVIATIONS

CBE, cyclobutene; BCB, benzocyclobutene; SMFS, single molecule force spectroscopy; FMPES, force-modified potential energy surface; CASSCF, complete-active-space self-consistent field; ENUE, effective number of unpaired electrons.

REFERENCES

(1) Woodward, R. B.; Hoffmann, R. The Conservation of Orbital Symmetry. *Angew. Chem., Int. Ed.* **1969**, *8*, 781-853.

(2) Bian, M.; Li, L.; Ding, H. Recent Advances on the Application of Electrocyclic Reactions in Complex Natural Product Synthesis. *Synthesis* **2017**, *49*, 4383-4413.

(3) Cooper, W.; Walters, W. D. The Thermal Isomerization of Cyclobutene1,2. *J. Am. Chem. Soc.* **1958**, *80*, 4220-4224.

(4) Frey, H. M. Thermal Unimolecular Isomerizations of Substituted Cyclobutenes. Part 2.—1,2-Dimethylcyclobutene. *Trans. Faraday Soc.* **1963**, *59*, 1619-1622.

(5) Blomquist, A. T.; LaLancette, E. A. Diphenylcyclobutadienoquinone. Iii.1 Attempted Synthesis of 1,2-Diphenylcyclobutadiene2. *J. Org. Chem.* **1964**, *29*, 2331-2334.

(6) Schlag, E. W.; Peatman, W. B. The Thermal Cyclization of Hexafluorobutadiene to Hexafluorocyclobutene. *J. Am. Chem. Soc.* **1964**, *86*, 1676-1679.

(7) Frey, H. M.; Pope, B. M.; Skinner, R. F. Thermal Isomerization of Cyclobutenes. Part 10.—3,3-Dimethylcyclobutene and 1,3,3-Trimethylcyclobutene. *Trans. Faraday Soc.* **1967**, *63*, 1166-1170.

(8) Pomerantz, M.; Hartman, P. H. Thermal Rearrangement of 3-Phenylcyclobutene. *Tetrahedron Lett.* **1968**, *9*, 991-993.

(9) Niwayama, S.; Kallel, E. A.; Spellmeyer, D. C.; Sheu, C.; Houk, K. N. Substituent Effects on Rates and Stereoselectivities of Conrotatory Electrocyclic Reactions of Cyclobutenes. A Theoretical Study. *J. Org. Chem.* **1996**, *61*, 2813-2825.

(10) Kirmse, W.; Rondan, N. G.; Houk, K. N. Stereoselective Substituent Effects on Conrotatory Electrocyclic Reactions of Cyclobutenes. *J. Am. Chem. Soc.* **1984**, *106*, 7989-7991.

(11) Spellmeyer, D. C.; Houk, K. N. Transition Structures of Pericyclic Reactions. Electron Correlation and Basis Set Effects on the Transition Structure and Activation Energy of the Electrocyclization of Cyclobutene to Butadiene. *J. Am. Chem. Soc.* **1988**, *110*, 3412-3416.

(12) Lee, P. S.; Zhang, X.; Houk, K. N. Origins of Inward Torquoselectivity by Silyl Groups and Other Σ-Acceptors in Electrocyclic Reactions of Cyclobutenes. *J. Am. Chem. Soc.* **2003**, *125*, 5072-5079.

(13) Klundt, I. L. Benzocyclobutene and Its Derivatives. *Chem. Rev.* **1970**, *70*, 471-487.

(14) Matsuya, Y.; Ohsawa, N.; Nemoto, H. Accelerated Electrocyclic Ring-Opening of Benzocyclobutenes under the Influence of a B-Silicon Atom. *J. Am. Chem. Soc.* **2006**, *128*, 412-413.

(15) Nava, P.; Carissan, Y. On the Ring-Opening of Substituted Cyclobutene to Benzocyclobutene: Analysis of Π Delocalization, Hyperconjugation, and Ring Strain. *Phys. Chem. Chem. Phys.* **2014**, *16*, 16196-16203.

(16) Lee, P. S.; Sakai, S.; Hörstermann, P.; Roth, W. R.; Kallel, E. A.; Houk, K. N. Altering the Allowed/Forbidden Gap in Cyclobutene Electrocyclic Reactions: Experimental and Theoretical Evaluations of the Effect of Planarity Constraints. *J. Am. Chem. Soc.* **2003**, *125*, 5839-5848.

(17) Sakai, S. Theoretical Studies on the Electrocyclic Reaction Mechanisms for S-Cis Butadiene and Disilylbutadiene. *Journal of Molecular Structure: THEOCHEM* **1999**, *461-462*, 283-295.

(18) Sakai, S. Theoretical Studies of the Electrocyclic Reaction Mechanisms of O-Xylylene to Benzocyclobutene. *J. Phys. Chem. A* **2000**, *104*, 11615-11621.

(19) Baldwin, J. E.; Andrist, A. H.; Pinschmidt, R. K. Orbital-Symmetry-Disallowed Energetically Concerted Reactions. *Acc. Chem. Res.* **1972**, *5*, 402-406.

(20) Brauman, J. I.; Archie, W. C. Energies of Alternate Electrocyclic Pathways. Pyrolysis of Cis-3,4-Dimethylcyclobutene. *J. Am. Chem. Soc.* **1972**, *94*, 4262-4265.

(21) Hickenboth, C. R.; Moore, J. S.; White, S. R.; Sottos, N. R.; Baudry, J.; Wilson, S. R. Biasing Reaction Pathways with Mechanical Force. *Nature* **2007**, *446*, 423-427.

(22) Ong, M. T.; Leiding, J.; Tao, H.; Virshup, A. M.; Martínez, T. J. First Principles Dynamics and Minimum Energy Pathways for Mechanochemical Ring Opening of Cyclobutene. *J. Am. Chem. Soc.* **2009**, *131*, 6377-6379.

(23) Ribas-Arino, J.; Shiga, M.; Marx, D. Unravelling the Mechanism of Force-Induced Ring-Opening of Benzocyclobutenes. *Chem.-Eur. J.* **2009**, *15*, 13331-13335.

(24) Ribas-Arino, J.; Shiga, M.; Marx, D. Understanding Covalent Mechanochemistry. *Angew. Chem., Int. Ed.* **2009**, *48*, 4190-4193.

(25) Kochhar, G. S.; Bailey, A.; Mosey, N. J. Competition between Orbitals and Stress in Mechanochemistry. *Angew. Chem., Int. Ed.* **2010**, *49*, 7452-7455.

(26) Ribas-Arino, J.; Shiga, M.; Marx, D. Mechanochemical Transduction of Externally Applied Forces to Mechanophores. *J. Am. Chem. Soc.* **2010**, *132*, 10609-10614.

(27) Dopieralski, P.; Anjukandi, P.; Rückert, M.; Shiga, M.; Ribas–Arino, J.; Marx, D. On the Role of Polymer Chains in Transducing External Mechanical Forces to Benzocyclobutene Mechanophores. *J. Mater. Chem.* **2011**, *21*, 8309-8316.

(28) Konda, S. S. M.; Brantley, J. N.; Bielawski, C. W.; Makarov, D. E. Chemical Reactions Modulated by Mechanical Stress: Extended Bell Theory. *J. Chem. Phys.* **2011**, *135*, 164103.

(29) Li, W.; Edwards, S. A.; Lu, L.; Kubar, T.; Patil, S. P.; Grubmüller, H.; Groenhof, G.; Gräter, F. Force Distribution Analysis of Mechanochemically Reactive Dimethylcyclobutene. *ChemPhysChem* **2013**, *14*, 2687-2697.

(30) Huang, Z.; Yang, Q.-Z.; Khvostichenko, D.; Kucharski, T. J.; Chen, J.; Boulatov, R. Method to Derive Restoring Forces of Strained Molecules from Kinetic Measurements. *J. Am. Chem. Soc.* **2009**, *131*, 1407-1409.

(31) Yang, Q.-Z.; Huang, Z.; Kucharski, T. J.; Khvostichenko, D.; Chen, J.; Boulatov, R. A Molecular Force Probe. *Nat. Nanotech.* **2009**, *4*, 302-306.

(32) Wang, J.; Kouznetsova, T. B.; Niu, Z.; Ong, M. T.; Klukovich, H. M.; Rheingold, A. L.; Martinez, T. J.; Craig, S. L. Inducing and Quantifying Forbidden Reactivity with Single-Molecule Polymer Mechanochemistry. *Nat. Chem.* **2015**, *7*, 323-327.

(33) Wang, J.; Kouznetsova, T. B.; Niu, Z.; Rheingold, A. L.; Craig, S. L. Accelerating a Mechanically Driven Anti-Woodward–Hoffmann Ring Opening with a Polymer Lever Arm Effect. *J. Org. Chem.* **2015**, *80*, 11895-11898.

(34) Izak-Nau, E.; Campagna, D.; Baumann, C.; Göstl, R. Polymer Mechanochemistry-Enabled Pericyclic Reactions. *Polym. Chem.* **2020**, *11*, 2274-2299.

(35) Hodge, P. Entropically Driven Ring-Opening Polymerization of Strainless Organic Macrocycles. *Chem. Rev.* **2014**, *114*, 2278-2312.

(36) Lenhardt, J. M.; Black Ramirez, A. L.; Lee, B.; Kouznetsova, T. B.; Craig, S. L. Mechanistic Insights into the Sonochemical Activation of Multimechanophore Cyclopropanated Polybutadiene Polymers. *Macromolecules* **2015**, *48*, 6396-6403.

(37) Klukovich, H. M.; Kouznetsova, T. B.; Kean, Z. S.; Lenhardt, J. M.; Craig, S. L. A Backbone Lever-Arm Effect Enhances Polymer Mechanochemistry. *Nat. Chem.* **2013**, *5*, 110-114.

(38) Wu, D.; Lenhardt, J. M.; Black, A. L.; Akhremitchev, B. B.; Craig, S. L. Molecular Stress Relief through a Force-Induced Irreversible Extension in Polymer Contour Length. *J. Am. Chem. Soc.* **2010**, *132*, 15936-15938.

(39) Kouznetsova, T. B.; Wang, J.; Craig, S. L. Combined Constant-Force and Constant-Velocity Single-Molecule Force Spectroscopy of the Conrotatory Ring Opening Reaction of Benzocyclobutene. *ChemPhysChem* **2017**, *18*, 1486-1489.

(40) Oberhauser, A. F.; Marszalek, P. E.; Erickson, H. P.; Fernandez, J. M. The Molecular Elasticity of the Extracellular Matrix Protein Tenascin. *Nature* **1998**, *393*, 181-185.

(41) Beyer, M. K. The Mechanical Strength of a Covalent Bond Calculated by Density Functional Theory. *J. Chem. Phys.* **2000**, *112*, 7307-7312.

(42) Klein, I. M.; Husic, C. C.; Kovács, D. P.; Choquette, N. J.; Robb, M. J. Validation of the Cogef Method as a Predictive Tool for Polymer Mechanochemistry. *J. Am. Chem. Soc.* **2020**, *142*, 16364-16381.

(43) Lee, C.; Yang, W.; Parr, R. G. Development of the Colle-Salvetti Correlation-Energy Formula into a Functional of the Electron Density. *Phys. Rev. B* **1988**, *37*, 785-789.

(44) Becke, A. D. Density-Functional Thermochemistry. Iii. The Role of Exact Exchange. *J. Chem. Phys.* **1993**, *98*, 5648-5652.

(45) Vosko, S. H.; Wilk, L.; Nusair, M. Accurate Spin-Dependent Electron Liquid Correlation Energies for Local Spin Density Calculations: A Critical Analysis. *Can. J. Phys.* **1980**, *58*, 1200-1211.

(46) Stephens, P. J.; Devlin, F. J.; Chabalowski, C. F.; Frisch, M. J. Ab Initio Calculation of Vibrational Absorption and Circular Dichroism Spectra Using Density Functional Force Fields. *J. Phys. Chem.* **1994**, *98*, 11623-11627.

(47) Hariharan, P. C.; Pople, J. A. The Influence of Polarization Functions on Molecular Orbital Hydrogenation Energies. *Theor. chim. acta* **1973**, *28*, 213-222.

(48) Chen, Z.; Zhu, X.; Yang, J.; Mercer, J. A. M.; Burns, N. Z.; Martinez, T. J.; Xia, Y. The Cascade Unzipping of Ladderane Reveals Dynamic Effects in Mechanochemistry. *Nat. Chem.* **2020**, *12*, 302-309.

(49) Head-Gordon, M. Characterizing Unpaired Electrons from the One-Particle Density Matrix. *Chem. Phys. Lett.* **2003**, *372*, 508-511.

(50) Tian, Y.; Cao, X.; Li, X.; Zhang, H.; Sun, C.-L.; Xu, Y.; Weng, W.; Zhang, W.; Boulatov, R. A Polymer with Mechanochemically Active Hidden Length. *J. Am. Chem. Soc.* **2020**, *142*, 18687-18697.

(51) Srinivasan, R. Thermal and Photochemical Isomerization of Cis-3,4-Dimethylcyclobutene. *J. Am. Chem. Soc.* **1969**, *91*, 7557-7561.

(52) Morales-Bayuelo, A. Understanding the Electronic Reorganization in the Thermal Isomerization Reaction of Trans-3,4-Dimethylcyclobutene. Origins of Outward Pseudodiradical {2n + 2π} Torquoselectivity. *Int. J. Quantum Chem.* **2013**, *113*, 1534-1543.

(53) Nixon, R.; De Bo, G. Three Concomitant C–C Dissociation Pathways During the Mechanical Activation of an N-Heterocyclic Carbene Precursor. *Nat. Chem.* **2020**, *12*, 826-831.

(54) Tian, Y. C.; Boulatov, R. Quantum-Chemical Validation of the Local Assumption of Chemomechanics for a Unimolecular Reaction. *Chemphyschem* **2012**, *13*, 2277-2281.

(55) Kean, Z. S.; Niu, Z.; Hewage, G. B.; Rheingold, A. L.; Craig, S. L. Stress-Responsive Polymers Containing Cyclobutane Core Mechanophores: Reactivity and Mechanistic Insights. *J. Am. Chem. Soc.* **2013**, *135*, 13598-13604.

(56) Ramirez, A. L. B.; Kean, Z. S.; Orlicki, J. A.; Champhekar, M.; Elsakr, S. M.; Krause, W. E.; Craig, S. L. Mechanochemical Strengthening of a Synthetic Polymer in Response to Typically Destructive Shear Forces. *Nat. Chem.* **2013**, *5*, 757-761.

(57) Wang, J.; Piskun, I.; Craig, S. L. Mechanochemical Strengthening of a Multi-Mechanophore Benzocyclobutene Polymer. *ACS Macro Lett.* **2015**, *4*, 834-837.

(58) Degen, C. M.; May, P. A.; Moore, J. S.; White, S. R.; Sottos, N. R. Time-Dependent Mechanochemical Response of Sp-Cross-Linked Pmma. *Macromolecules* **2013**, *46*, 8917-8921.

(59) Lee, C. K.; Beiermann, B. A.; Silberstein, M. N.; Wang, J.; Moore, J. S.; Sottos, N. R.; Braun, P. V. Exploiting Force Sensitive Spiropyrans as Molecular Level Probes. *Macromolecules* **2013**, *46*, 3746-3752.

(60) Gossweiler, G. R.; Hewage, G. B.; Soriano, G.; Wang, Q.; Welshofer, G. W.; Zhao, X.; Craig, S. L. Mechanochemical Activation of Covalent Bonds in Polymers with Full and Repeatable Macroscopic Shape Recovery. *ACS Macro Lett.* **2014**, *3*, 216-219.

(61) Grady, M. E.; Beiermann, B. A.; Moore, J. S.; Sottos, N. R. Shockwave Loading of Mechanochemically Active Polymer Coatings. *ACS Appl. Mater. Interfaces* **2014**, *6*, 5350-5355.

(62) Imato, K.; Irie, A.; Kosuge, T.; Ohishi, T.; Nishihara, M.; Takahara, A.; Otsuka, H. Mechanophores with a Reversible Radical System and Freezing-Induced Mechanochemistry in Polymer Solutions and Gels. *Angew. Chem., Int. Ed.* **2015**, *54*, 6168-6172.

(63) Lin, Y.; Kouznetsova, T. B.; Craig, S. L. A Latent Mechanoacid for Time-Stamped Mechanochromism and Chemical Signaling in Polymeric Materials. *J. Am. Chem. Soc.* **2020**, *142*, 99-103.

(64) Diesendruck, C. E.; Steinberg, B. D.; Sugai, N.; Silberstein, M. N.; Sottos, N. R.; White, S. R.; Braun, P. V.; Moore, J. S. Proton-Coupled Mechanochemical Transduction: A Mechanogenerated Acid. *J. Am. Chem. Soc.* **2012**, *134*, 12446-12449.